

Cerebral and cerebellar grey matter atrophy in Friedreich ataxia: the IMAGE-FRDA study

Louisa P. Selvadurai¹ · Ian H. Harding¹ · Louise A. Corben^{1,2,3} · Monique R. Stagnitti¹ · Elsdon Storey⁴ · Gary F. Egan^{1,5} · Martin B. Delatycki^{1,2,3,6} · Nellie Georgiou-Karistianis¹

Received: 10 May 2016/Revised: 30 July 2016/Accepted: 30 July 2016/Published online: 13 August 2016
© Springer-Verlag Berlin Heidelberg 2016

Abstract Friedreich ataxia (FRDA) is traditionally associated with neuropathology in the cerebellar dentate nucleus and spinal cord. Growing evidence also suggests involvement of the cerebral and cerebellar cortices, although reports of structural abnormalities remain mixed. This study assessed the structural integrity of cortical grey matter in FRDA, focussing on regions in which pathology may underlie the motor deficits characteristic of this disorder. T1-weighted anatomical magnetic resonance imaging scans were acquired from 31 individuals with FRDA and 37 healthy controls. Cortical thickness (FreeSurfer) and cortical volume (SPM-VBM) were measured in cerebral motor regions-of-interest (primary motor, dorsal and ventral premotor, and supplementary motor areas)

alongside unconstrained exploratory analyses of the cerebral and cerebellar cortices. Correlations were assessed between cortical thickness/volume measures and each of disease severity, length of the causative genetic triplet-repeat expansion, and finger-tapping behavioural measures. Individuals with FRDA had significantly reduced cortical thickness, relative to controls, in the premotor and supplementary motor areas. Reduced cortical thickness and/or volume were also observed in the cuneus and precuneus, posterior aspects of the medial and lateral prefrontal cortices, insula, temporal poles, and cerebellar lobules V, VI, and VII. Measures of clinical severity, genetic abnormality, and motor dysfunction correlated with volume loss in the lateral cerebellar hemispheres. These results suggest that atrophy preferentially affects premotor relative to primary areas of the cortical motor system, and also extends to a range of non-motor brain regions. Furthermore, cortical thickness and cortical volume findings were largely divergent, suggesting that each is sensitive to different aspects of neuropathology in FRDA. Overall, this study supports a disease model involving neural aberrations within the cerebral and cerebellar cortices, beyond those traditionally associated with this disorder.

L. P. Selvadurai and I. H. Harding contributed equally to this work.

Electronic supplementary material The online version of this article (doi:10.1007/s00415-016-8252-7) contains supplementary material, which is available to authorized users.

✉ Ian H. Harding
ian.harding@monash.edu

¹ School of Psychological Sciences and Monash Institute of Cognitive and Clinical Neurosciences, Monash University, 18 Innovation Walk, Melbourne, VIC 3800, Australia

² Bruce Lefroy Centre for Genetic Health Research, Murdoch Childrens Research Institute, Melbourne, Australia

³ Department of Paediatrics, The University of Melbourne, Melbourne, Australia

⁴ Department of Medicine, Monash University, Melbourne, Australia

⁵ Monash Biomedical Imaging, Monash University, Melbourne, Australia

⁶ Clinical Genetics, Austin Health, Melbourne, Australia

Keywords Friedreich ataxia · MRI · Cortical thickness · Voxel-based morphometry

Introduction

Friedreich ataxia (FRDA), the most common inherited ataxia, is primarily characterised by progressive incoordination of limb movements and gait [30]. The causative genetic mutation is most often a homozygous GAA repeat expansion in the *FXN* gene, leading to deficient expression

of the frataxin protein and subsequent degeneration of neural, cardiac, and endocrine tissues [30]. Canonical sites of neuropathology include the dentate nuclei of the cerebellum, dorsal root ganglia, and various spinal tracts [30]. Dentate pathology is thought to contribute to gait and limb ataxia, dysarthria, and dysphagia [23], while corticospinal tract damage accounts for secondary motor features, including muscle weakness and abnormal reflexes [30].

Evidence for cerebral involvement in FRDA is also growing. Using in vivo neuroimaging, abnormalities in cerebral activation have been reported in association with motor and cognitive performance [1, 17]. Reduced structural integrity has also been observed in white matter tracts linking the cerebellum and cerebral cortex [2, 44], and cerebral components of the spinal tracts [10, 32]. Recent anatomical investigations further support subcortical grey matter atrophy in the basal ganglia, midbrain, and thalamus [18, 32]. Finally, observed behavioural deficits in higher order cognitive functions, including motor planning [8] and cognitive control [20], may be best accounted for by the combination of cerebellar and cerebral disruptions.

Despite evidence of cerebral contributions to FRDA, reports of structural changes in the cerebral cortex remain mixed. Using whole-brain voxel-based morphometry (VBM) and cortical thickness measures, Rezende and colleagues [32] reported a loss of grey matter principally in motor areas. Conversely, two other VBM studies did not find evidence of cerebral grey matter changes, although much smaller sample sizes were employed [9, 13]. It, therefore, remains uncertain whether functional disruptions in the cerebrum are solely the consequence of reduced inputs from the cerebellum/spinal cord (i.e., functional diaschisis; [7]), or if anatomical changes in the cerebrum, putatively reflecting neuronal death or loss of neuropil, also contribute. With respect to the latter, it is noteworthy that clinically relevant cerebral grey matter atrophy has been reported in other inherited ataxias [19, 34].

As motor dysfunctions are the most salient clinical features of FRDA, the integrity of the cerebral motor system may be particularly relevant. In vivo functional abnormalities have been consistently reported within the supplementary motor areas across motor tasks of varying complexity, alongside more varied evidence of dorsal premotor and primary motor involvement [1, 15]. In the cerebellum, reported anatomical and functional abnormalities are principally weighted towards the lateral hemispheres, [1, 32] which preferentially interact with the premotor and prefrontal cortices of the cerebrum [6]. These findings together motivate our hypothesis that premotor areas may be disproportionately impacted relative to the primary motor system.

This study aimed to assess the structural integrity of the motor cortex in individuals with FRDA by examining cortical volume and cortical thickness using a region-of-interest (ROI) approach. The ROIs comprised the four main subcomponents of the cortical motor system (dorsal and ventral premotor, supplementary motor, and primary motor areas), as identified by a meta-analysis of functional MRI in motor tasks [26]. Whole-brain analyses were also performed. Relationships between cortical structure and clinical metrics, including disease severity, length of the GAA repeat expansion, and performance on simple finger-tapping motor tasks were assessed.

Methods

Participants

Data analyses included 31 individuals homozygous for a GAA expansion in intron one of *FXN* and 37 age- and gender-matched healthy controls (Table 1) recruited through the Melbourne-based IMAGE-FRDA neuroimaging study. Data were collected between August 2013 and August 2014. Two additional individuals with FRDA were excluded due to excessive movement during scanning ($n = 1$) and evidence of gross cerebral atrophy, an unusual finding in FRDA ($n = 1$). Participants had no history of psychiatric or neurologic disorders, apart from FRDA. Disease severity was quantified using the Friedreich Ataxia Rating Scale (FARS) [39]. The study was sanctioned by the Monash Health Human Research Ethics Committee. All participants provided written informed consent.

Motor tasks

Participants performed speeded and self-paced finger tapping tasks [38]. During speeded tapping, participants pressed a button with their non-dominant index finger as rapidly as possible for 10 s, followed by a 10 s rest period, repeated five times. The average inter-tap interval (ms) was recorded for subsequent between-group and correlational analyses (Table 1). During self-paced tapping, participants alternated between pressing two buttons, one with each thumb, in time with a repeated tone presented every 550 ms (1.8 Hz). After 11 taps, the tone ceased and participants were required to maintain the same pace for an additional 31 taps. This procedure was repeated five times. Tapping precision was calculated as the inverse of the standard deviation of the difference between observed and correct inter-tap intervals (Table 1); this precision value was used for subsequent between-group and correlational analyses [38].

Table 1 Demographic, clinical, and behavioural measures

	FRDA (<i>N</i> = 31)	Controls (<i>N</i> = 37)	Statistic	<i>p</i> value
Demographics				
Age (years)	36.58 ± 13.00	37.09 ± 12.87	$t_{66} = 0.16$	0.872
Gender (M, F)	17, 14	20, 17	$\chi^2 = 0.04$	0.948
Clinical data				
FARS score	80.92 ± 28.39	–	–	–
BDI-II score	8.23 ± 8.42	4.97 ± 5.79	$t_{66} = 1.88$	0.065
Disease duration (years)	16.91 ± 9.53	–	–	–
Age at onset (years)	19.55 ± 8.82	–	–	–
GAA ₁ repeat length	546 ± 225	–	–	–
GAA ₂ repeat length	865 ± 253	–	–	–
Finger tapping performance				
Speeded inter-tap interval (ms)	495.1 ± 183.9	209.0 ± 27.6	$t_{65} = 9.23$	<0.001
Paced tapping (precision)	11.13 ± 4.70	21.81 ± 6.19	$t_{65} = 7.80$	<0.001

Values are mean ± SD

FARS Friedreich Ataxia Rating Scale; *BDI-II* Beck Depression Inventory-II [5]; *disease duration* age when tested minus age at disease onset; *age at onset* age at which first symptom was reported; *GAA* length of the GAA repeat in intron 1 of the *FXN* gene in the smaller (GAA₁) and larger (GAA₂) alleles

Magnetic resonance imaging

Whole-brain magnetic resonance imaging was conducted using a 3-Tesla Siemens Skyra scanner with a 32-channel head coil. High-resolution T1-weighted magnetization-prepared rapid gradient-echo (MPRAGE) images were acquired over 3.5 min: TR = 1900 ms, TE = 2.19 ms, flip = 9°, FOV = 256 × 256 mm, 176 sagittal slices, and 1.0 mm isotropic voxels.

Grey matter measurement

Cortical thickness

Surface-based cortical thickness analysis was conducted using the semi-automated FreeSurfer pipeline (Version 5.3) [11]. In brief, following removal of non-brain tissues, models of the grey matter–white matter boundary and the grey matter–CSF boundary are constructed. Cortical thickness is defined as the distance between these boundaries at each vertex (point) across the cortical surface. All images were inspected to ensure accuracy of the surface models. Any errors, most often due to dura mater being mislabelled as grey matter, were manually corrected according to current best practice (<https://surfer.nmr.mgh.harvard.edu>). Cortical thickness assessments can only be undertaken in the cerebrum (not cerebellum).

Cortical volume

Volume-based assessments were undertaken using VBM12 (<http://www.neuro.uni-jena.de/vbm>) and SPM12 software

(<http://www.fil.ion.ucl.ac.uk/spm/>) to perform a standard VBM analysis [3]. The T1-weighted images were first segmented into tissue subclasses (grey matter/white matter/CSF) and normalised to standard space using a non-linear diffeomorphic deformation (DARTEL). The grey matter segmentations were then adjusted (modulated) using the non-linear component of the deformation field. Overall differences in brain size are discounted at this stage, negating the need for further correction during statistical modelling. A 5 and 10 mm full-width-half-maximum (FWHM) Gaussian spatial smoothing kernel was then applied to the cerebellar and cerebral images, respectively. Analysis included both the cerebral and cerebellar cortices; subcortical volume changes are reported elsewhere [18].

Region-of-interest definition

The primary motor (M1), dorsal premotor (PMd), ventral premotor (PMv), and supplementary motor areas (SMA) were defined by the Human Motor Area Template (HMAT; Fig. 1a), a volume-based atlas constructed using a meta-analysis of functional MRI in cortical motor areas [26]. Mean cortical thickness and grey matter volume within each ROI were extracted for each participant.

Statistical analyses

Statistical inference was undertaken using SPSS Statistics 22 (IBM Corp.). For each of cortical thickness and cortical volume, between-group differences were assessed using analysis of covariance (ANCOVA). Four two-way mixed model ANCOVAs (one for each of M1, PMd,

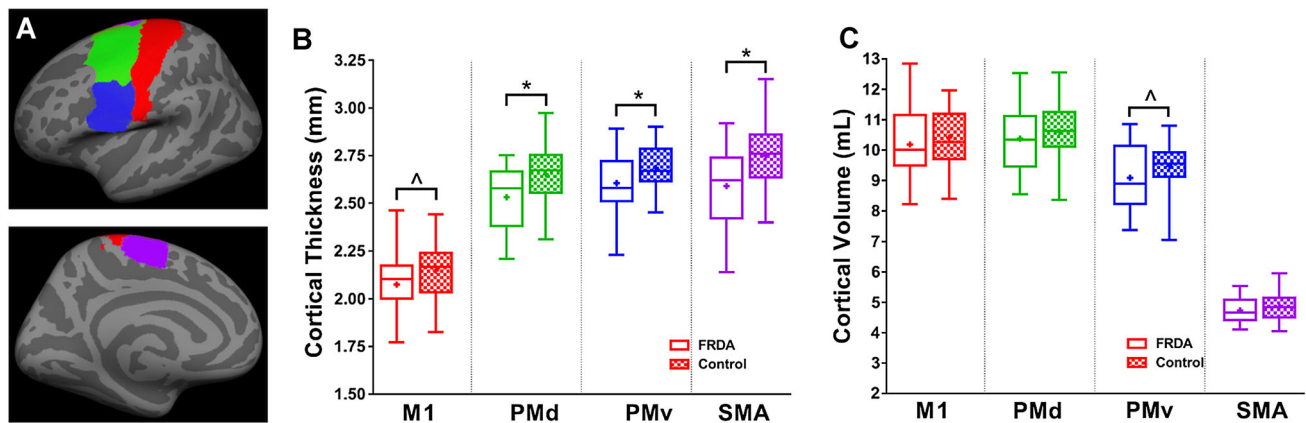


Fig. 1 Group comparisons (FRDA vs. controls) in the motor regions-of-interest (**a**) for cortical thickness (**b**) and cortical volume (**c**). * $p < 0.013$ (corrected $p < 0.05$), $^{\wedge}p < 0.05$ (uncorrected). *M1*

PMv, and SMA) were conducted, with a between-subjects factor of GROUP (FRDA, Controls) and a within-subjects factor of HEMISPHERE (left, right). Hemisphere was included as a factor of non-interest to account for potential hemispheric differences. Age and gender were entered as covariates. Significance thresholds were Bonferroni-corrected across the four regions-of-interest ($p < 0.013$); uncorrected trends ($p < 0.05$) are also reported for comprehensiveness.

Exploratory analyses were also conducted across the whole cerebrum for thickness and volume; and separately across the whole cerebellum for volume. Thickness at each vertex and volume at each voxel were compared between the FRDA and control groups using random-effects general linear modelling, implemented in Freesurfer and SPM, respectively. Age and gender were included as covariates. Inference on cortical thickness effects, including correction of statistical thresholds for multiple comparisons, was achieved using Monte Carlo cluster simulations for cortical thickness (cluster-level FWE-corrected $p < 0.05$; cluster-forming threshold, $p < 0.01$; 10,000 permutations) [16]. For cortical volume measures, threshold-free cluster enhancement (TFCE; [36]) and non-parametric permutation testing were employed (TFCE-level FWE-corrected $p < 0.05$). Correction was undertaken separately for the cerebrum and the cerebellum.

Correlation analyses were conducted to assess the linear associations between cortical thickness/volume and each of the: (1) FARS scores, (2) GAA repeat sizes of the smaller *FXN* allele (GAA_1), (3) speeded tapping rates, and (4) paced tapping precision in the FRDA cohort. For each individual, mean cortical thickness and cortical volume were extracted for each ROI and each significant cluster identified in the relevant exploratory analysis. For each region, a Pearson correlation was conducted between mean cortical thickness and each of the variables listed

primary motor area; *PMd* dorsal premotor area; *PMv* ventral premotor area; *SMA* supplementary motor area

above, and separately for cortical volume and each of these variables. Bonferroni correction was undertaken across four ROIs and, separately, the number of significant clusters.

Furthermore, linear correlations with each variable across the whole cortex were explored by fitting a simple linear regression to each cortical thickness vertex and each cortical volume voxel, separately for each clinical/behavioural variable. Statistical thresholds were corrected for multiple comparisons using the same methods as described above (Monte Carlo simulations for thickness, TFCE for volume).

Results

Motor regions-of-interest

Significant reductions in cortical thickness in the FRDA cohort, relative to controls (main effects of GROUP), were evident in the PMd ($p = 0.002$), PMv ($p = 0.002$) and SMA ($p = 0.001$); Fig. 1b; Table 2. Trend-level reduction was observed in M1 ($p = 0.048$).

There were no significant group differences in grey matter volume at the corrected threshold. A trend towards reduced volume in the FRDA cohort in the PMv ($p = 0.022$) was observed; Fig. 1c; Table 2.

Notably, all effects (whether significant, trending, or insignificant) were in the direction of decreased volume or thickness in the FRDA cohort.

For both cortical thickness and cortical volume, the ANCOVAs revealed no significant GROUP by HEMISPHERE interaction in M1 [thickness: $F(1,64) = 0.04$, $p = 0.849$, volume: $F(1,64) = 0.62$, $p = 0.433$], PMd [$F(1,64) = 2.58$, $p = 0.113$, $F(1,64) = 3.52$, $p = 0.065$], PMv [$F(1,64) = 0.002$, $p = 0.962$, $F(1,64) = 0.84$,

Table 2 Cortical thickness and volume in motor regions-of-interest

ROI	Cortical thickness (mm ± SEM)				Cortical volume (mL ± SEM)			
	FRDA	Control	<i>F</i> (1,64)	<i>p</i>	FRDA	Control	<i>F</i> (1,64)	<i>p</i>
M1	2.07 ± 0.03	2.15 ± 0.03	4.61	0.036	10.18 ± 0.17	10.42 ± 0.15	1.11	0.30
PMd	2.53 ± 0.03	2.64 ± 0.02	10.02	0.002	10.37 ± 0.16	10.62 ± 0.14	1.39	0.24
PMv	2.60 ± 0.02	2.68 ± 0.02	9.48	0.003	9.08 ± 0.13	9.49 ± 0.12	5.54	0.022
SMA	2.59 ± 0.04	2.75 ± 0.03	11.36	0.001	4.74 ± 0.08	4.86 ± 0.07	1.27	0.26

Bold *p* values, corrected-level *p* < 0.05

M1 primary motor cortex; *PMd* dorsal premotor cortex; *PMv* ventral premotor cortex; *SMA* supplementary motor area

p = 0.363], or SMA [*F*(1,64) = 1.44, *p* = 0.234, *F*(1,64) = 0.06, *p* = 0.813]. Therefore, inference was restricted to the main effect of GROUP.

Cerebral exploratory analysis

Cortical thickness was significantly reduced in FRDA relative to controls in the bilateral paracentral lobules (overlapping with the SMA ROI), bilateral temporal poles, right ventrolateral prefrontal cortex (PFC) and anterior insula, and right precuneus (Fig. 2a; Online Resource 1, Supplementary Table 1).

Cortical volume was significantly reduced in the bilateral frontal operculum and posterior aspects of the lateral PFC (overlapping with the PMv ROI), left pre-SMA, and

right cuneus/precuneus (Fig. 2b; Online Resource 1, Supplementary Table 2).

Overlap in reduced thickness and volume was evident in the right precuneus. There was no evidence of increased thickness or volume in FRDA.

Cerebellar exploratory analysis

Reduced grey matter volume in the FRDA group, relative to controls, was evident throughout the lateral cerebellar hemispheres bilaterally (Fig. 3a; Online Resource 1, Supplementary Table 3). These differences encompassed much of Lobules VI and neighbouring regions of Crus I, areas of Crus II, and Lobule VIIb. Medial to Lobule VI, reduced grey matter was also evident in Lobule V, particularly in

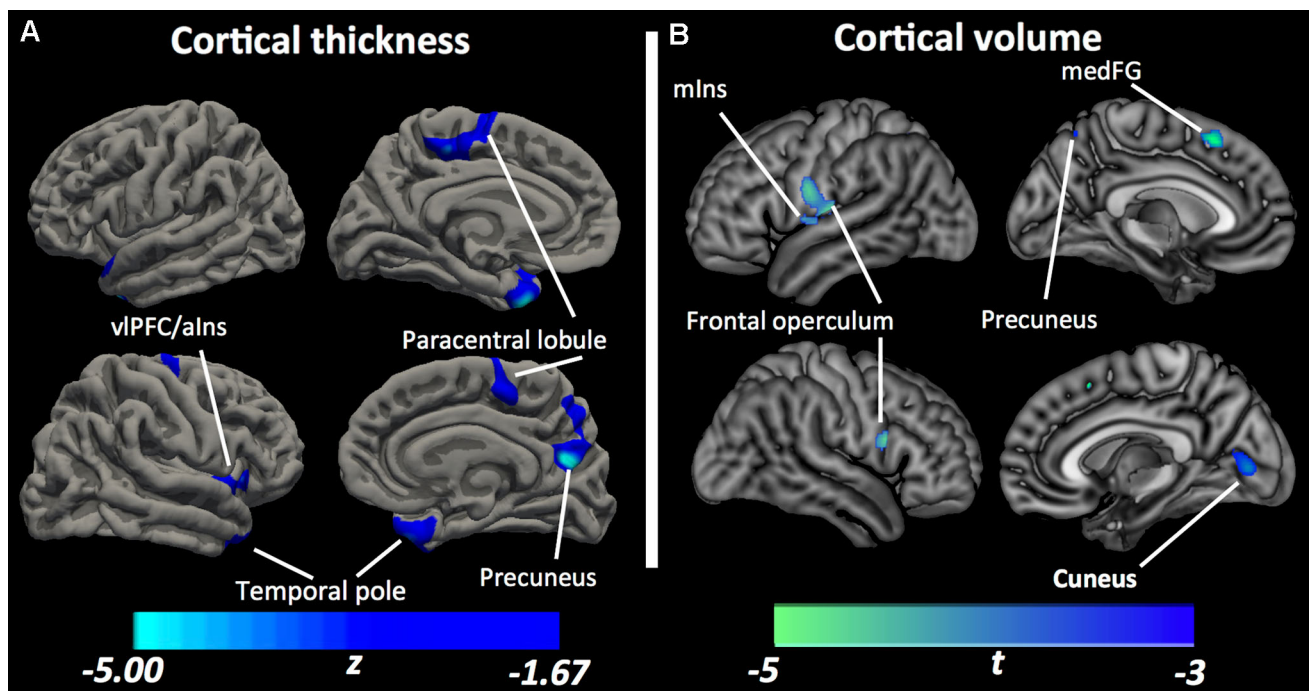
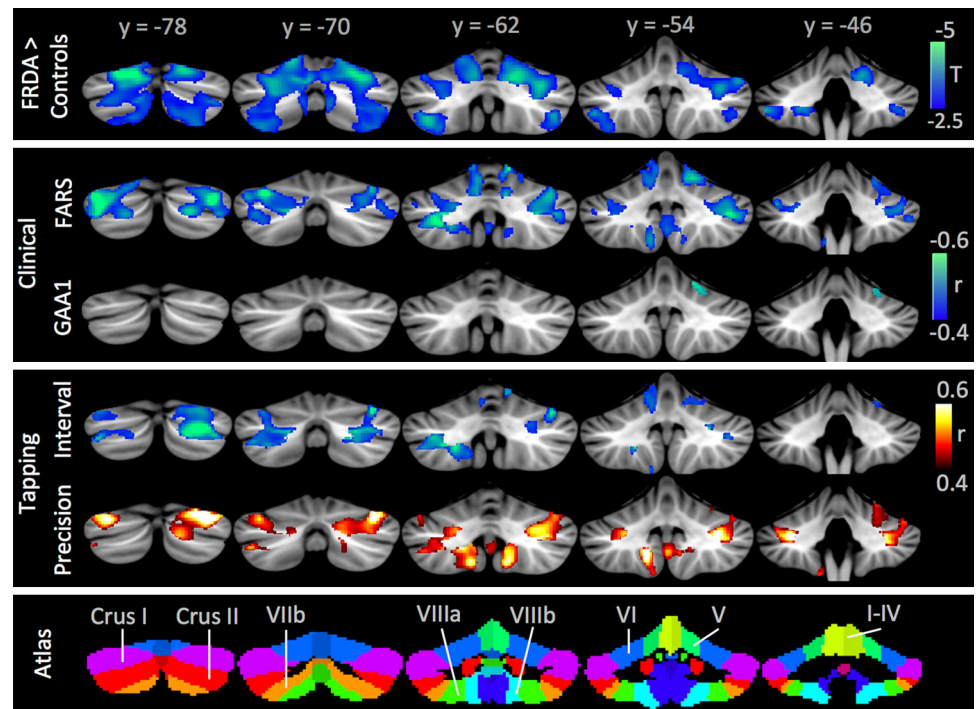


Fig. 2 Results of cerebral exploratory analysis of cortical thickness (a; cluster-level FWE-corrected *p* < 0.05) and cortical volume (b; threshold-free cluster enhancement FWE-corrected *p* < 0.05). Blue =

FRDA < controls. *vIPFC* ventrolateral prefrontal cortex; *alns* anterior insula; *mIns* middle insula; *medFG* medial frontal gyrus

Fig. 3 Cerebellar volume differences. Areas with significantly less grey matter in FRDA relative to controls (*top*; *blue* = FRDA < control) and significant correlations with clinical and finger tapping measures (middle; *blue* = negative, *red* = positive). The SUI cerebellar atlas is provided for reference (*bottom*; modified from [22] under CC BY-NC license). All effects meet FWE-corrected $p < 0.05$ significance using threshold-free cluster enhancement and are presented in MNI space



the right hemisphere. No significant effects were observed in vermal regions. There was no evidence of increased volume in FRDA.

Clinical and behavioural correlations

Clinical and behavioural correlations with cerebellar grey matter volume are shown in Fig. 3. Associations with disease severity were evident across Lobules V–VII, while GAA1 correlations were restricted to right Lobule VI. Speeded tapping interval mapped onto Crus I and II, and paced tapping precision onto Crus I and Lobules VIIIb/IX. In all cases, poorer clinical, genetic, and behavioural indices were associated with less grey-matter volume (Fig. 3; Online Resource 1, Supplementary Fig. 1; Online Resource 1, Supplementary Table 4).

There were no significant correlations with clinical/behavioural measures and cerebral grey matter volume or thickness.

Discussion

In this study, we report structural abnormalities in the cerebral and cerebellar grey matter in individuals with FRDA, relative to healthy controls. Reduced thickness and volume of grey matter in the cerebral cortex were observed in motor (PMd, PMv, and SMA) and non-motor areas (cuneus, precuneus, anterior temporal cortex, insula, and posterior aspects of the medial and lateral PFC). Volumetric

analysis of the cerebellum replicated and extended previous findings of grey matter loss, with particular weighting towards the lateral hemispheres [32]. Cerebellar, but not cerebral, grey matter measures were significantly associated with clinical severity, genetic markers, and motor performance in individuals with FRDA.

Grey matter loss in the motor system in FRDA is consistent with reported aberrations in motor-related functional activations [1, 15], reduced white matter connectivity with lower brain areas [2, 44], and another recent report of cortical grey matter atrophy [32]. The current results support the hypothesis that cerebral functional changes are not only the consequence of reduced cerebello-cerebral neural signalling, but that neuronal death or loss of neuropil in the cerebrum itself may also contribute. Furthermore, this study provides evidence of differential atrophy in subregions of the motor system, with preferential involvement of premotor regions (PMd, PMv, and SMA). This observation is consistent with cerebellar degeneration that is preferentially targeted to the lateral hemispheres, which primarily interact with the premotor and prefrontal cerebrum [6]. Conversely, the relatively spared cerebellar vermal and paravermal fields preferentially interact with the relatively spared primary motor system.

Grey matter loss in extra-motor regions of the cerebral cortex was also identified. Of these regions, only abnormalities in the insula have previously been reported in FRDA, including aberrant functional activation and functional connectivity [1, 14, 17]. However, extra-motor

involvement is consistent with growing evidence of cognitive deficits in FRDA, including impaired cognitive control [20], verbal fluency [28], visuoperception, and visuoconstruction [29]. However, assessing potential links between grey matter loss in non-motor cortical areas and non-motor FRDA phenomenology will require further research.

One compelling possibility for effects in a number of the non-motor areas identified in this study relates to their status as ‘hub’ regions within key functional brain networks; in other words, regions with a high level of interconnectivity with other brain areas [37]. In particular, the insula is a hub region in the salience network and the precuneus is a hub region in the default mode network [27, 40]. The temporal pole also displays hub characteristics [21]. Hub regions are known to be particularly vulnerable to the impact of primary disease consequences or secondary spread from primary sites of pathology [37, 41] and both the salience and default mode networks have been implicated in FRDA in the previous functional imaging work [1, 14, 15]. These results may thus provide further evidence of the impact of FRDA on large-scale cortical networks (e.g. [17]).

Our findings also indicate a differential sensitivity of cortical volume and thickness measurements to FRDA-related pathology. First, only the cortical thickness analyses were sensitive to statistically significant group differences in motor ROIs. Second, the pattern of volume and thickness differences revealed in the exploratory analyses were largely divergent, with overlap restricted to the medial parietal lobe. This divergence has previously been observed in both health and disease [25, 35, 43], and discrepancies between volumetric and thickness findings are not unexpected, as these measures are not necessarily directly related to each other. Indeed, it appears that changes in cortical volume are better accounted for by changes in cortical *surface area* than changes in cortical thickness [22]. Furthermore, cortical thickness and cortical surface area have different genetic bases, are thought to arise from different cellular processes [31], and show different topological profiles in the human brain [33]. The influence of cortical curvature and grey matter/white matter contrast may also partly drive volume–thickness discrepancies [25]. Taken together, cortical thickness and cortical volume likely measure different aspects of cerebral grey matter [42], although the specific cellular correlates of each remain a matter of ongoing research.

This study adds to the current evidence of supra-tentorial structural involvement in FRDA. However, while both cerebral and cerebellar grey matter changes are evident, significant associations with clinical severity, genetic loading, and motor dysfunction are observed only in the latter. Significant clinical correlations in cerebellar, but not cerebral, structures are also reported in other recent

structural and functional studies of the brain in FRDA, [17, 32] consistent with cerebellar effects being the most robust and reliable indices of brain pathology in this disorder [24]. As with the between-group differences, these correlation effects were weighted to lobules VI and VII, providing further evidence that neural disruptions in the lateral hemispheres—areas more typically associated with premotor and cognitive functions—are particularly relevant to FRDA morbidity.

Conversely, anatomical-clinical associations did not manifest in the cerebrum. We speculate that these more subtle anatomical changes may be insufficient to induce functional consequences owing to local capacity reserve or compensation within alternative systems [4, 12]. Moreover, clinical and behavioural measures that conflate many aspects of the disorder or cognitive-behavioural processes—such as the FARS and finger tapping—may be insufficiently sensitive to subtle neurological changes. Finally, insufficient statistical power to detect significant correlations in this work also cannot be ruled out. Thus, although a growing body of literature supports the replicability of anatomical abnormalities in the cerebrum, their clinical consequences remain an ongoing question.

The a priori ROI and exploratory approaches applied in this study each have inherent limitations. ROI analyses provide increased power to detect relatively small effect sizes (due to decreased multiple comparisons), but relatively poor spatial specificity due to inclusion of large areas of cortex; the opposite is true of exploratory approaches. This inherent trade-off is exemplified by the exploratory detection of volume differences in subregions of the PMv, which manifest only as trend-level group differences across the whole structure. Our combined analysis approach attempts to offset these reciprocal strengths/weaknesses.

In conclusion, this study supports the existence of structural abnormalities in the cerebral and cerebellar cortices in FRDA. Tissue atrophy is preferentially observed in premotor areas of the cortical motor system, alongside a number of ‘hub’ regions of non-motor networks. Overall, this work adds to a growing literature illustrating pathology in regions distal from the cerebellum and spinal cord, thereby representing a move towards a more complete model of neuropathology in FRDA.

Acknowledgments Funding support was provided by the Australian National Health and Medical Research Council (Project Grant 1046037). We thank Dr. Dominic Dwyer and Dr. Sarah Whittle for technical consultations.

Compliance with ethical standards

Conflicts of interest The authors declare that they have no conflict of interest.

References

- Akhlaghi H, Corben L, Georgiou-Karistianis N, Bradshaw J, Delatycki MB, Storey E, Egan GF (2012) A functional MRI study of motor dysfunction in Friedreich's ataxia. *Brain Res* 1471:138–154
- Akhlaghi H, Yu J, Corben L, Georgiou-Karistianis N, Bradshaw JL, Storey E, Delatycki MB, Egan GF (2014) Cognitive deficits in Friedreich ataxia correlate with micro-structural changes in dentatorubral tract. *Cerebellum* 13:187–198
- Ashburner J, Friston KJ (2000) Voxel-based morphometry—the methods. *NeuroImage* 11:805–821
- Barulli D, Stern Y (2013) Efficiency, capacity, compensation, maintenance, plasticity: emerging concepts in cognitive reserve. *Trends Cogn Sci* 17:502–509. doi:10.1016/j.tics.2013.1008.1012
- Beck AT, Steer RA, Brown GK (1996) Manual for the BDI-II. The Psychological Corporation, San Antonio
- Buckner RL, Krienen FM, Castellanos A, Diaz JC, Yeo BTT (2011) The organization of the human cerebellum estimated by intrinsic functional connectivity. *J Neurophysiol* 106:2322–2345
- Carrera E, TONI G (2014) Diaschisis: past, present, future. *Brain J Neurol* 137:2408–2422
- Corben LA, Delatycki MB, Bradshaw JL, Churchyard AJ, Georgiou-Karistianis N (2011) Utilisation of advance motor information is impaired in Friedreich ataxia. *Cerebellum* 10:793–803
- Della Nave R, Ginestroni A, Giannelli M, Tessa C, Salvatore E, Salvi F, Dotti MT, De Michele G, Piacentini S, Mascalchi M (2008) Brain structural damage in Friedreich's ataxia. *J Neurol Neurosurg Psychiatry* 79:82–85
- Della Nave R, Ginestroni A, Tessa C, Salvatore E, Bartolomei I, Salvi F, Dotti MT, De Michele G, Piacentini S, Mascalchi M (2008) Brain white matter tracts degeneration in Friedreich ataxia. An in vivo MRI study using tract-based spatial statistics and voxel-based morphometry. *NeuroImage* 40:19–25
- Fischl B, Dale AM (2000) Measuring the thickness of the human cerebral cortex from magnetic resonance images. *Proc Natl Acad Sci* 97:11050–11055
- Fornito A, Zalesky A, Breakspear M (2015) The connectomics of brain disorders. *Nat Rev Neurosci* 16:159–172
- Franca MC Jr, D'Abreu A, Yasuda CL, Bonadia LC, Santos da Silva M, Nucci A, Lopes-Cendes I, Cendes F (2009) A combined voxel-based morphometry and 1H-MRS study in patients with Friedreich's ataxia. *J Neurol* 256:1114–1120
- Georgiou-Karistianis N, Akhlaghi H, Corben LA, Delatycki MB, Storey E, Bradshaw JL, Egan GF (2012) Decreased functional brain activation in Friedreich ataxia using the Simon effect task. *Brain Cogn* 79:200–208
- Ginestroni A, Diciotti S, Cecchi P, Pesaresi I, Tessa C, Giannelli M, Nave RD, Salvatore E, Salvi F, Dotti MT, Piacentini S, Soricelli A, Cosottini M, De Stefano N, Mascalchi M (2012) Neurodegeneration in Friedreich's ataxia is associated with a mixed activation pattern of the brain. A fMRI study. *Hum Brain Mapp* 33:1780–1791
- Hagler DJ Jr, Saygin AP, Sereno MI (2006) Smoothing and cluster thresholding for cortical surface-based group analysis of fMRI data. *NeuroImage* 33:1093–1103
- Harding IH, Corben LA, Storey E, Egan GF, Stagnitti MR, Poudel G, Delatycki MB, Georgiou-Karistianis N (2016) Frontocerebellar dysfunction and dysconnectivity underlying cognitive functioning in Friedreich ataxia: the IMAGE-FRDA study. *Hum Brain Mapp* 37:338–350
- Harding IH, Raniga P, Delatycki MB, Stagnitti MR, Corben LA, Storey E, Georgiou-Karistianis N, Egan GF (2016) Tissue atrophy and elevated iron concentration in the extrapyramidal motor system in Friedreich ataxia: the IMAGE-FRDA study. *J Neurol Neurosurg Psychiatry*. doi:10.1136/jnnp-2015-312665
- Hernandez-Castillo CR, Galvez V, Diaz R, Fernandez-Ruiz J (2016) Specific cerebellar and cortical degeneration correlates with ataxia severity in spinocerebellar ataxia type 7. *Brain Imaging Behav* 10:252–257
- Hocking DR, Corben LA, Fielding J, Cremer PD, Millist L, White OB, Delatycki MB (2014) Saccade reprogramming in Friedreich ataxia reveals impairments in the cognitive control of saccadic eye movement. *Brain Cogn* 87:161–167
- Hwang K, Hallquist MN, Luna B (2012) The development of hub architecture in the human functional brain network. *Cereb Cortex* 23:2380–2393
- Im K, Lee J-M, Lyttelton O, Kim SH, Evans AC, Kim SI (2008) Brain size and cortical structure in the adult human brain. *Cereb Cortex* 18:2181–2191
- Koeppen AH, Davis AN, Morral JA (2011) The cerebellar component of Friedreich's ataxia. *Acta Neuropathol* 122:323–330
- Koeppen AH, Mazurkiewicz JE (2013) Friedreich ataxia: neuropathology revised. *J Neuropathol Exp Neurol* 72:78–90
- Kong L, Herold CJ, Zöllner F, Salat DH, Lässer MM, Schmid LA, Fellhauer I, Thomann PA, Essig M, Schad LR, Erickson KI, Schröder J (2015) Comparison of grey matter volume and thickness for analysing cortical changes in chronic schizophrenia: a matter of surface area, grey/white matter intensity contrast, and curvature. *Psychiatry Res Neuroimaging* 231:176–183
- Mayka MA, Corcos DM, Leurgans SE, Vaillancourt DE (2006) Three-dimensional locations and boundaries of motor and premotor cortices as defined by functional brain imaging: a meta-analysis. *NeuroImage* 31:1453–1474
- Menon V, Uddin LQ (2010) Saliency, switching, attention and control: a network model of insula function. *Brain Struct Funct* 214:655–667
- Nachbauer W, Bodner T, Boesch S, Karner E, Eigentler A, Neier L, Benke T, Delazer M (2014) Friedreich ataxia: executive control is related to disease onset and GAA repeat length. *Cerebellum* 13:9–16
- Nieto A, Correia R, de Nobrega E, Montón F, Hess S, Barroso J (2012) Cognition in Friedreich ataxia. *Cerebellum* 11:834–844
- Pandolfo M (2009) Friedreich ataxia: the clinical picture. *J Neurol* 256:3–8
- Panizzon MS, Fennema-Notestine C, Eyler LT, Jernigan TL, Prom-Wormley E, Neale M, Jacobson K, Lyons MJ, Grant MD, Franz CE, Xian H, Tsuang M, Fischl B, Seidman L, Dale A, Kremen WS (2009) Distinct genetic influences on cortical surface area and cortical thickness. *Cereb Cortex (New York, NY)* 19:2728–2735
- Rezende TJR, Silva CB, Yassuda CL, Campos BM, D'Abreu A, Cendes F, Lopes-Cendes I, França MC (2016) Longitudinal magnetic resonance imaging study shows progressive pyramidal and callosal damage in Friedreich's ataxia. *Mov Disord* 31:70–78
- Sanabria-Diaz G, Melie-García L, Iturria-Medina Y, Alemán-Gómez Y, Hernández-González G, Valdés-Urrutia L, Galán L, Valdés-Sosa P (2010) Surface area and cortical thickness descriptors reveal different attributes of the structural human brain networks. *NeuroImage* 50:1497–1510
- Schulz JB, Borkert J, Wolf S, Schmitz-Hübsch T, Rakowicz M, Mariotti C, Schoels L, Timmann D, van de Warrenburg B, Dürr A, Pandolfo M, Kang J-S, Mandly AG, Nägele T, Grisoli M, Boguslawska R, Bauer P, Klockgether T, Hauser T-K (2010) Visualization, quantification and correlation of brain atrophy with clinical symptoms in spinocerebellar ataxia types 1, 3 and 6. *NeuroImage* 49:158–168
- Silk TJ, Beare R, Malpas C, Adamson C, Vilgis V, Vance A, Bellgrove MA (2016) Cortical morphometry in attention deficit/

- hyperactivity disorder: contribution of thickness and surface area to volume. *Cortex* 82:1–10
36. Smith SM, Nichols TE (2009) Threshold-free cluster enhancement: addressing problems of smoothing, threshold dependence and localisation in cluster inference. *NeuroImage* 44:83–98
 37. Sporns O, Honey CJ, Kötter R (2007) Identification and classification of hubs in brain networks. *PLoS One* 2:e1049
 38. Stout JC, Paulsen JS, Queller S, Solomon AC, Whitlock KB, Campbell JC, Carlozzi N, Duff K, Beglinger LJ, Langbehn DR, Johnson SA, Biglan KM, Aylward EH (2011) Neurocognitive signs in prodromal Huntington disease. *Neuropsychology* 25:1–14
 39. Subramony SH, May W, Lynch D, Gomez C, Fischbeck K, Hallett M, Taylor P, Wilson R, Ashizawa T (2005) Measuring Friedreich ataxia: interrater reliability of a neurologic rating scale. *Neurology* 64:1261–1262
 40. Tomasi D, Volkow ND (2011) Functional connectivity hubs in the human brain. *NeuroImage* 57:908–917
 41. van den Heuvel MP, Sporns O (2013) Network hubs in the human brain. *Trends Cognit Sci* 17:683–696
 42. Winkler AM, Kochunov P, Blangero J, Almasy L, Zilles K, Fox PT, Duggirala R, Glahn DC (2010) Cortical thickness or grey matter volume? the importance of selecting the phenotype for imaging genetics studies. *NeuroImage* 53:1135–1146
 43. Yang J-J, Kwon H, Lee J-M (2016) Complementary characteristics of correlation patterns in morphometric correlation networks of cortical thickness, surface area, and gray matter volume. *Sci Reports* 6:26682
 44. Zalesky A, Akhlaghi H, Corben LA, Bradshaw JL, Delatycki MB, Storey E, Georgiou-Karistianis N, Egan GF (2014) Cerebello-cerebral connectivity deficits in Friedreich ataxia. *Brain Struct Funct* 219:969–981